Investigation of the sulfur doping profile in femtosecond-laser processed silicon

Kay-Michael Guenther, Thomas Gimpel, Stefan Kontermann, and Wolfgang Schade

Citation: Applied Physics Letters **102**, 202104 (2013); doi: 10.1063/1.4807679
View online: http://dx.doi.org/10.1063/1.4807679
View Table of Contents: http://scitation.aip.org/content/aip/journal/apl/102/20?ver=pdfcov
Published by the AIP Publishing

Investigation of the sulfur doping profile in femtosecond-laser processed silicon

Kay-Michael Guenther,[1,a)] Thomas Gimpel,[2] Stefan Kontermann,[2] and Wolfgang Schade[2]
[1]*Clausthal University of Technology, EFZN, Am Stollen 19B, 38640 Goslar, Germany*
[2]*Fraunhofer Heinrich Hertz Institute, Am Stollen 19B, 38640 Goslar, Germany*

(Received 26 March 2013; accepted 6 May 2013; published online 22 May 2013)

In this letter, we demonstrate that silicon can be doped with electrically active sulfur donors beyond the solubility limit of $3 \times 10^{16}\,\mathrm{cm}^{-3}$. We investigate the sulfur doping profile at the surface of femtosecond-laser processed silicon with secondary ion mass spectroscopy (SIMS) and capacitance-voltage measurements. SIMS confirms previous observations that the fs-laser process can lead to a sulfur hyperdoping of $5 \times 10^{19}\,\mathrm{cm}^{-3}$ at the surface. Nevertheless, the electrical measurements show that less than 1% of the sulfur is electrically active as a donor. © *2013 AIP Publishing LLC*. [http://dx.doi.org/10.1063/1.4807679]

Irradiating silicon with femtosecond-laser pulses can lead to a structuring of the surface in the micro- and nanometer scale.[1] In dependence on the irradiation parameters, smooth wafer-like structures as well as sharp conical spikes are possible.[2] This material is called black silicon due to its strongly reduced reflectance.[3]

If the laser process is performed under a sulfur hexafluoride (SF_6) containing atmosphere, sulfur is incorporated into the silicon surface and leads to an enhanced absorption below the bandgap due to sulfur related interband states.[4] Previous investigations with energy dispersive X-ray emission spectroscopy and secondary ion mass spectroscopy (SIMS) indicate a sulfur concentration of roughly 1% ($\sim 10^{20}\,\mathrm{cm}^{-3}$) at the surface.[2,5] This value exceeds the maximum solid solubility of sulfur in silicon ($3 \times 10^{16}\,\mathrm{cm}^{-3}$)[6] by four orders of magnitude. Sulfur supplies several band gap states,[7] ranging from mid-gap[8] to donor states.[6,9] Therefore, when the laser process is performed on a p-type substrate, a pn-junction is formed. A working solar cell, solely based on this black silicon material with a sulfur emitter was successfully demonstrated with an efficiency of $\eta \approx 4.5\%$.[10]

In this letter, we investigate the sulfur doping profile of fs-laser doped silicon with SIMS and electrical impedance measurements. The concentration of the electrically active donor states is measured with capacitance-voltage (CV) spectroscopy. This technique evaluates the capacitance C of a reversed-biased Schottky diode in dependence of the applied DC bias voltage V_{DC}. The effective doping density N_d can be calculated from[11]

$$N_d(V_{DC}) = \pm \frac{2}{q\varepsilon_r\varepsilon_0 A^2 \mathrm{d}(1/C^2)/\mathrm{d}V_{DC}}, \qquad (1)$$

with the Schottky contact area A, the electron charge q, the dielectric constant of the vacuum ε_0, and of the semiconductor material ε_r.

Two samples are fabricated from (100) monocrystalline floatzone silicon substrates. The base material is boron doped (1–5 Ω cm) and the native oxide was removed by a 15 min dip in hydrofluoric acid. The laser process is performed with a commercially available Mantis oscillator as seed laser from Coherent and a Spitfire regenerative amplifier from Spectra Physics with a repetition rate of 10 kHz at a wavelength of 800 nm and fluencies of $E \approx 20\,\mathrm{kJ/m^2}$. The silicon is irradiated with five pulses per spot to create a medium structured surface, which is called grey silicon.[10] Sample A is processed under ambient air and serves as a reference sample. Sample B is processed under SF_6 atmosphere ($p = 0.66$ bar). For the electrical measurements, two rectangular Schottky contacts, with area sizes of 4.84 mm^2 and 31.8 mm^2 are fabricated on samples A and B, respectively, by sputter coating 50 nm titanium followed by 150 nm gold through a shadow mask.

We use a Hiden Analytical secondary ion mass spectrometer with 3 keV primary caesium ions to investigate the concentration profile of the incorporated sulfur atoms. To calculate the sulfur concentration from the mass spectrometer counts, we fabricated a reference silicon sample by implanting a peak sulfur concentration of $10^{20}\,\mathrm{cm}^{-3}$ at a depth of 430 nm.

Figure 1 displays the sulfur concentration profiles for samples A and B as well as the reference sample. Sample B exhibits a maximum sulfur atom concentration of $5 \times 10^{19}\,\mathrm{cm}^{-3}$ in the top 100 nm. This is roughly 0.1 at. % and lower than the value reported by Crouch *et al.*[2] Nevertheless, sample B contains three orders of magnitude more sulfur than the solubility limit ($3 \times 10^{16}\,\mathrm{cm}^{-3}$).[6]

Sample A and the reference sample show a sulfur signal in the range of $2 \times 10^{18}\,\mathrm{cm}^{-3}$ at the surface. We believe that this is associated with surface contaminations, possibly originating from sulfur hexafluoride residues in the laboratory atmosphere. Because this phenomenon is limited to the top ten nanometers of the samples, interference on the electrical measurements is not expected.

For the measurement of the capacitance C, we evaluate the impedance spectra of the Schottky contact as we described in our previous work.[12] In short, we evaluate impedance spectra by using suitable equivalent circuits to extract capacitance voltage characteristics for each present depletion region. This method has the advantage to give an accurate value for the capacitance, even when additional space charges are present. This is the case for our samples,

a)Electronic mail: kay-michael.guenther@efzn.de. Telephone: +49 5321 6855 170.

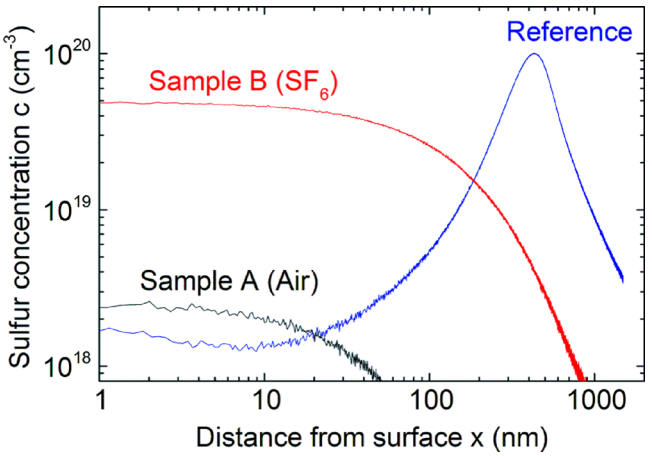

FIG. 1. Sulfur concentration depth profile measured with SIMS. A reference silicon sample (ion implanted sulfur with a peak concentration of $10^{20}\,\mathrm{cm}^{-3}$ at a distance of 430 nm from the surface) is used to calibrate the signal counts.

because a structured, amorphous layer at the surface[13,14] as well as a pn-junction is present.

In this work, we evaluate the impedance of two co-planar Schottky contacts, which are placed on the structured and sulfur doped surface. This results in a series combination of at least the two Schottky barriers at low bias voltages and the pn junction at larger voltages. Therefore, we use a series combination of an ohmic resistance R and a number of shunted constant phase elements (CPEs) for the equivalent circuit. A CPE is a non-intuitive, generalized, frequency-dependent circuit element.[15] Its impedance is

$$Z_{CPE}(\omega) = q^{-1}(i\omega)^{-n}, \tag{2}$$

with the angular frequency $\omega = 2\pi f$ and the imaginary unit $i = \sqrt{-1}$.[15] The CPE exponent n accounts for the phase shift.[15] The physical meaning of the CPE changes with the value of n between capacitance ($n = 1$), resistance ($n = 0$), and inductance ($n = -1$).[15] Accordingly, the factor q identifies with a capacitance C for $n = 1$ and with a conductivity R^{-1} for $n = 0$.[15] For values of n between 0 and 1, the CPE can be interpreted as a mixture of a resistor and a capacitance.[15] The "real" capacitance of the space charge region can be calculated with[16]

$$C = q^{\frac{1}{n}} R^{\frac{1-n}{n}}, \tag{3}$$

R being the respective shunt resistance.

The reason for using CPEs instead of simple capacities is that a CPE is able to account for contact interface roughness[17] as it is present with the laser structured surface of the black silicon material. The findings of Rammelt *et al.*[17] suggest that for $0.5 \leq n \leq 1$, the fractal dimension D of the metal-semiconductor interface can be calculated with

$$D = \frac{n+1}{n}. \tag{4}$$

Figure 2 shows the measured reactance spectra in dependence of the applied DC bias voltage for sample B. We use an equivalent circuit with three R-CPE combinations to fit the measured data

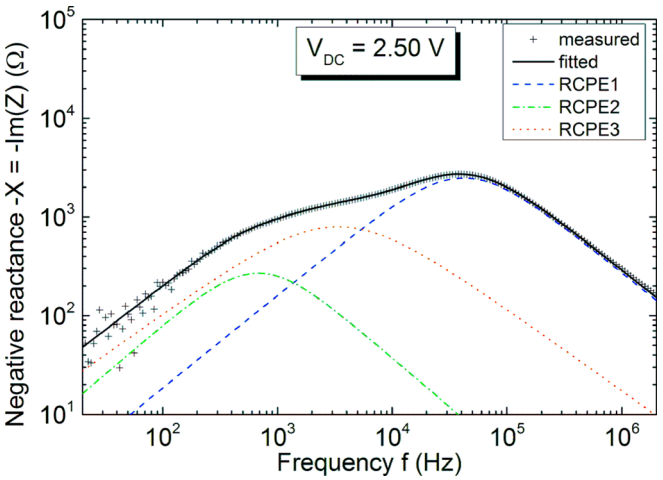

FIG. 2. Measured reactance spectrum (crosses) and fitted equivalent circuit (black line) for sample B (processed under SF_6 ambient) in dependence of the applied DC voltage. The individual R-CPE combinations from the equivalent circuit are displayed in colored, broken lines (enhanced online) [URL: http://dx.doi.org/10.1063/1.4807679.1].

$$Z_{fit}(\omega) = R_s + \sum_{k=1}^{3}\left[\frac{1}{R_k} + q_k(i\omega)^{n_k}\right]. \tag{5}$$

As it can be seen in Fig. 2, at 2.5 V bias voltage the high frequency R-CPE combination marked as RCPE1 is the dominant part of the spectrum, exhibiting the largest resistance. Therefore, it can be attributed to the small contact's depletion zone, which is highly extended for large positive voltages in this setup. RCPE2 and RCPE3 are most likely attributed to the large contact which is in strong accumulation and minor space charges originating from an oxide layer or defects at the surface. Hence, for the determination of the doping concentration, we evaluate the capacitance of the depleted Schottky contact by using Eq. (3) on the fitted parameters of Eq. (5). The same procedure is performed on sample A and the results are displayed in a Mott-Schottky plot in Fig. 3.

Obviously, the slopes for both samples differ for voltages <0.6 V. Despite the ambient gas, both samples are processed

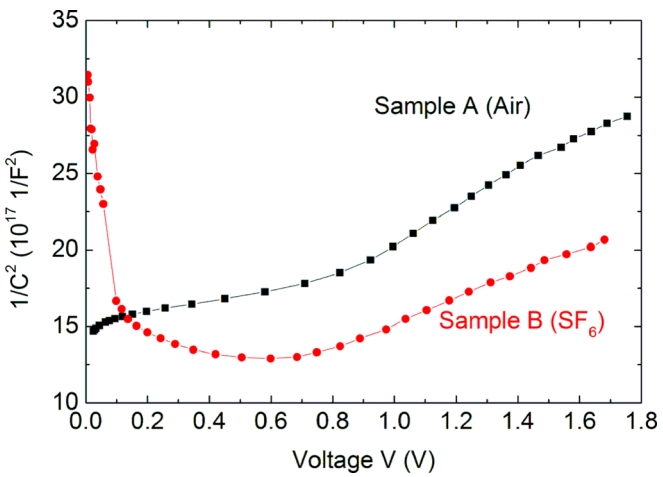

FIG. 3. Mott-Schottky plot for samples A and B as extracted from the fitted impedance spectra.

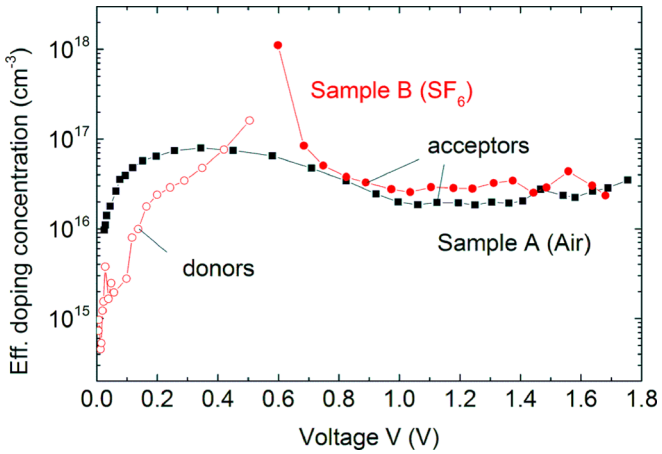

FIG. 4. Calculated effective doping concentrations for samples A and B. Donors are marked with open symbols.

identically and the contacts have the same size. Therefore, any difference results from incorporated sulfur donors. According to Eq. (1), a reversed slope represents a change in the effective doping type. Hence, evaluating the Mott-Schottky plot for the doping concentration in Fig. 4 reveals an effective donor concentration of 10^{15} to $10^{17}\,\mathrm{cm}^{-3}$.

It is known that the intersection of space charge regions can lead to false CV characteristics and apparently higher doping concentrations.[18] This can be observed at 0.6 V, where the Schottky contact's depletion region intersects with the pn junction. Close to the surface, the depletion layer is susceptible to influences by space charges related to the surface. Nevertheless, an effective donor concentration greater than $3 \times 10^{16}\,\mathrm{cm}^{-3}$ is verifiable. Hence, the base boron doping of at least $2.5 \times 10^{15}\,\mathrm{cm}^{-3}$ is compensated meaning that a sulfur donor concentration above the solubility limit ($3 \times 10^{16}\,\mathrm{cm}^{-3}$) is present.

The acceptor concentration for both samples lies consistently in the upper range of the base boron doping range ($2.5 \times 10^{15} \ldots 1.5 \times 10^{16}\,\mathrm{cm}^{-3}$) as reported by the wafer manufacturer or above. Secondary electron microscopic (SEM) images in Fig. 5 show that the laser structuring leads to a significant surface increase, which is not considered when the contact area is taken as A in Eq. (1). The surface could be increased by a factor of three and the resulting acceptor concentration would still be in the lower limit of the base doping range. In fact, the assumption that the resulting acceptor concentration is increased by the roughened surface is additionally supported by the SEM images, when the sizes of the surface structures of both samples are compared. As it can be seen, the presence of the sulfuric atmosphere seems to increase the roughness of the resulting surface of sample B. This agrees with the apparent acceptor concentrations in Fig. 4. Although both samples are fabricated from the same kind of silicon substrate and, therefore, we would expect to measure the same acceptor concentration in the bulk material, the determined values for sample B are slightly higher than for sample A (see Fig. 4 for $V > 0.7$ V). Further investigations in this matter are required and a more precise knowledge of the contact's interface area would refine the CV analysis' results. From another point of view, our results give a rough estimation for the surface increase.

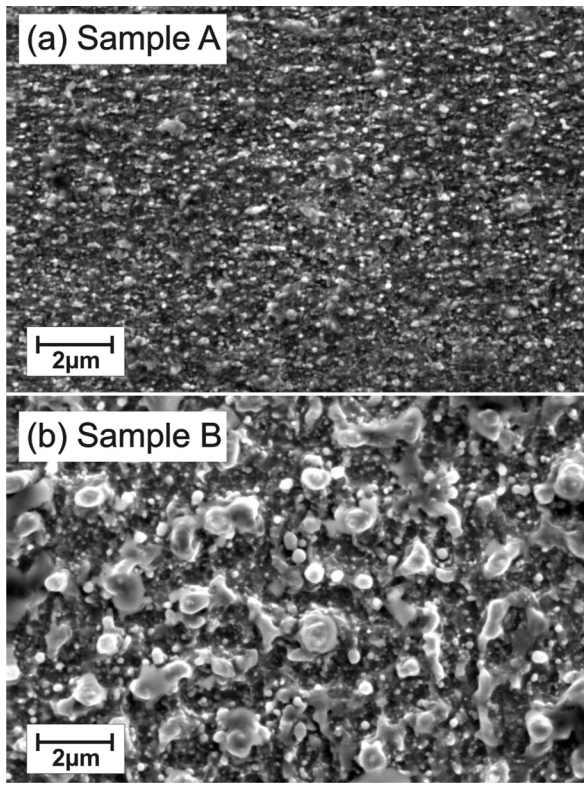

FIG. 5. Secondary electron microscope images of (a) sample A and (b) sample B.

The CPE's exponent n ranges from 0.956 to 0.977, which can be interpreted by using Eq. (4) as a fractal dimension of the interface in the range from 2.046 to 2.023.

The capacitance of the Schottky contact can be used to calculate the depth w of the respective depletion layer with $w = \varepsilon_0 \varepsilon_r A/C$ by assuming a plate capacitor.[11] If this is used here, the donor concentration is measured in a depth w between 570 and 890 nm. Compared with the SIMS measurement, this would mean that the CV results describe a region where the sulfur concentration decreases rapidly, not exceeding $2 \times 10^{18}\,\mathrm{cm}^{-3}$. Based on this assumption, less than 1% of the incorporated sulfur atoms act as a donor.

This estimated depth of the CV profiling range would agree with the spatial profiling limit for Schottky diodes, which is based on the Debye length and, therefore, depends on the doping concentration.[11] For doping concentrations in the range of 10^{16} to $10^{17}\,\mathrm{cm}^{-3}$, this limit is at a few hundred nanometers.[11] Hence, it is not possible to measure the donor concentration closer to the surface by using CV measurements with a Schottky contact. Nevertheless, we want to point out that a higher effective donor concentration in the region closer to the surface would lead to a lower Debye length[11] enabling the CV profiling in this region. Because this is not the case, we assume that the effective donor concentration does not exceed $10^{17}\,\mathrm{cm}^{-3}$ in the region, where SIMS measures a sulfur atom concentration of $5 \times 10^{19}\,\mathrm{cm}^{-3}$. Therefore, it is most likely that the donor supplying fraction of the sulfur atoms is even below 0.2%.

A CV profiling closer to the surface could be possible by using metal-insulator-semiconductor (MIS) structures instead of Schottky contacts.[11] Unfortunately, the fabrication of well

defined insulator layers for MIS devices on the laser structured surface is a challenging task and not yet investigated.

In summary, we studied silicon samples, which were structured by femtosecond-laser pulses under a SF_6 ambient. With SIMS, we confirmed earlier results that sulfur is incorporated in concentrations above the solubility limit. Additionally, we measured the electrically active sulfur donor concentration with capacitance-voltage spectroscopy and revealed that less than 1% of the sulfur atoms act as a donor. Nevertheless, we could demonstrate a sulfur donor doping of silicon beyond the solubility limit.

The authors like to thank Michal Schulz from the Clausthal University of Technology, Institute of Energy Research and Physical Technologies, for assisting with the SIMS measurements and Carsten Ronning from the University of Jena, Institute for Solid State Physics, for the fabrication of the ion implanted SIMS reference samples.

[1]T.-H. Her, R. J. Finlay, C. Wu, S. Deliwala, and E. Mazur, Appl. Phys. Lett. **73**, 1673 (1998).
[2]C. H. Crouch, J. E. Carey, M. Shen, E. Mazur, and F. Y. Génin, Appl. Phys. A **79**, 1635 (2004).
[3]J. Fang, C.-S. Chen, F. Wang, and S.-H. Liu, Chin. Phys. B **20**, 074202 (2011).
[4]C. Wu, C. H. Crouch, L. Zhao, J. E. Carey, R. J. Younkin, J. Levinson, E. Mazur, R. M. Farrel, P. Gothoskar, and A. Karger, Appl. Phys. Lett. **78**, 1850 (2001).
[5]R. Younkin, J. E. Carey, E. Mazur, J. A. Levinson, and C. M. Friend, J. Appl. Phys. **93**, 2626 (2003).
[6]R. O. Carlson, R. N. Hall, and E. M. Pell, J. Phys. Chem. Solids **8**, 81 (1959).
[7]Y. Mo, M. Z. Bazant, and E. Kaxiras, Phys. Rev. B **70**, 205210 (2004).
[8]H. G. Grimmeiss, E. Janzén, and B. Skarstam, J. Appl. Phys. **51**, 4212 (1980).
[9]E. Janzén, R. Stedman, G. Grossmann, and H. G. Grimmeiss, Phys. Rev. B **29**, 1907 (1984).
[10]S. Kontermann, A. L. Baumann, T. Gimpel, K.-M. Guenther, A. Ruibys, U. Willer, and W. Schade, MRS Proceedings **1405**, mrsf11-1405-y03-03 (2012).
[11]D. K. Schroder, *Semiconductor Material and Device Characterization* (John Wiley & Sons, New Jersey, 2006), pp. 61–109.
[12]K.-M. Guenther, H. Witte, A. Krost, S. Kontermann, and W. Schade, Appl. Phys. Lett. **100**, 042101 (2012).
[13]C. H. Crouch, J. E. Carey, J. M. Warrender, M. J. Aziz, E. Mazur, and F. Y. Génin, Appl. Phys. Lett. **84**, 1850 (2004).
[14]T. Gimpel, I. Höger, F. Falk, W. Schade, and S. Kontermann, Appl. Phys. Lett. **101**, 111911 (2012).
[15]X.-Z. Yuan, C. Song, H. Wang, and J. Zhan, *Electrochemical Impedance Spectroscopy in PEM Fuel Cells* (Springer, London, 2010), pp. 141–142.
[16]C. H. Hsu and F. Mansfeld, Corrosion **57**, 747 (2001).
[17]U. Rammelt and G. Reinhard, Electrochim. Acta **35**, 1045–1049 (1990).
[18]K. Lehovec, Appl. Phys. Lett. **26**, 82–84 (1975).